Bulletin of Scientific Contribution
GEOLOGY

Fakultas Teknik Geologi
UNIVERSITAS PADJADJARAN
homepage: http://jurnal.unpad.ac.id/bsc
p-ISSN: 1693-4873; e-ISSN: 2541-514X

Volume 24, No.01
April 2026

GEOCHEMISTRY OF VOLCANIC ROCKS OF THE BALEENDAH AREA AND SURROUNDINGS, BANDUNG REGENCY, WEST JAVA

Rinaldi Ikhram[1], Emir Sulaiman Ranuwijaya[1], Kurnia Arfiansyah Fachrudin[1]
[1]Geological Engineering Study Programme, Faculty of Geological Engineering, Universitas Padjadjaran, Bandung, Indonesia
*Email: rinaldi.ikhram@unpad.ac.id

ABSTRACT

Late Cenozoic arc magmatism in the Bandung Basin, West Java, records the chemical evolution of subduction-related volcanism along the Sunda arc. This study investigates the geochemistry of volcanic rocks from the second eruptive phase of Baleendah Volcano (~2.8–3.2 Ma), exposed in the Baleendah area, Bandung Regency. Major-oxide and trace element XRF analyses of four representative samples (ESR 02, ESR 14, ESR 18, ESR 22) yield SiO_2 contents of 57.6–63.3 wt.%, classifying the rocks as andesite on the Total Alkali–Silica diagram. On the SiO_2–K_2O diagram, all samples fall within the medium-K calc-alkaline field, consistent with their subduction-related origin. The FeOt/MgO vs. SiO_2 and AFM diagrams place the suite in a tholeiitic to transitional field (FeOt/MgO = 4.65–9.45). Harker variation diagrams record systematic decreases in Al_2O_3, CaO, MgO, and FeOt with increasing SiO_2, consistent with fractional crystallisation of plagioclase, pyroxene, and Fe–Ti oxides. Compared to the Pliocene KRM–CPN calc-alkaline suite from the same region, the ESR samples show lower MgO, CaO, Sr, V, and Co alongside higher FeOt/MgO ratios, indicating a more evolved, iron-enriched magma. These features collectively point to advanced fractional crystallisation under low oxygen fugacity within a shallow crustal magma chamber beneath the Baleendah volcanic system.

Keywords: Baleendah; andesite; tholeiitic; geochemistry; fractional crystallisation; Sunda arc

ABSTRAK

Magmatisme busur Kenozoikum Akhir di Cekungan Bandung, Jawa Barat, merekam evolusi kimia vulkanisme berkaitan subduksi di sepanjang busur Sunda. Penelitian ini mengkaji geokimia batuan vulkanik fase erupsi kedua Gunung Api Baleendah (~2,8–3,2 juta tahun lalu), yang tersingkap di daerah Baleendah, Kabupaten Bandung. Analisis XRF oksida utama dan unsur jejak pada empat sampel representatif (ESR 02, ESR 14, ESR 18, ESR 22) menghasilkan kandungan SiO_2 sebesar 57,6–63,3 %berat, mengklasifikasikan batuan sebagai andesit pada diagram Total Alkali–Silika. Pada diagram SiO_2–K_2O, seluruh sampel berada dalam lapangan kalk-alkalin medium-K, konsisten dengan asal-usul magma berkaitan subduksi. Diagram FeOt/MgO vs. SiO_2 dan diagram AFM menempatkan suite ini pada lapangan tholeitik hingga transisional (FeOt/MgO = 4,65–9,45). Diagram variasi Harker menunjukkan penurunan sistematis Al_2O_3, CaO, MgO, dan FeOt seiring peningkatan SiO_2, konsisten dengan fraksinasi kristal plagioklas, piroksen, dan mineral oksida Fe–Ti. Dibandingkan dengan suite kalk-alkalin Pliosen KRM–CPN dari kawasan yang sama, sampel ESR menunjukkan MgO, CaO, Sr, V, dan Co yang lebih rendah disertai rasio FeOt/MgO yang lebih tinggi, mengindikasikan magma yang lebih terdiferensiasi dan lebih kaya besi. Keseluruhan fitur ini secara kolektif menunjukkan fraksinasi kristal lanjut pada kondisi fugasitas oksigen rendah di dalam dapur magma kerak dangkal di bawah sistem vulkanik Baleendah.

Kata Kunci : Baleendah; andesit; tholeitik; geokimia; fraksinasi kristal; busur Sunda.

INTRODUCTION

Volcanic rocks record the chemical signature of sub-surface magmatic processes. Through geochemical analysis, the composition of the parental magma, magma series, and differentiation mechanisms that produce the spectrum of igneous rock compositions can be elucidated (Wilson, 1989; Best, 2013). Despite the broader characterisation of late Cenozoic magmatism in the Bandung Basin by Sunardi and Kimura (1998), the specific geochemical character of the Baleendah

volcanic phase remains poorly constrained. Understanding the magma series affinity and petrogenetic evolution of this phase is important for reconstructing the temporal development of Southern Bandung magmatism.

The Baleendah area and surroundings, Baleendah District, Bandung Regency, West Java, is a hilly terrain underlain by volcanic rocks from Baleendah Volcano (Figure 1). This extinct volcano underwent several eruptive phases; the second phase, occurring approximately 2.80–3.20 million years ago, produced andesitic lava flows now exposed at Gunung Geulis and Gunung Koromong (Bronto et al., 2006).

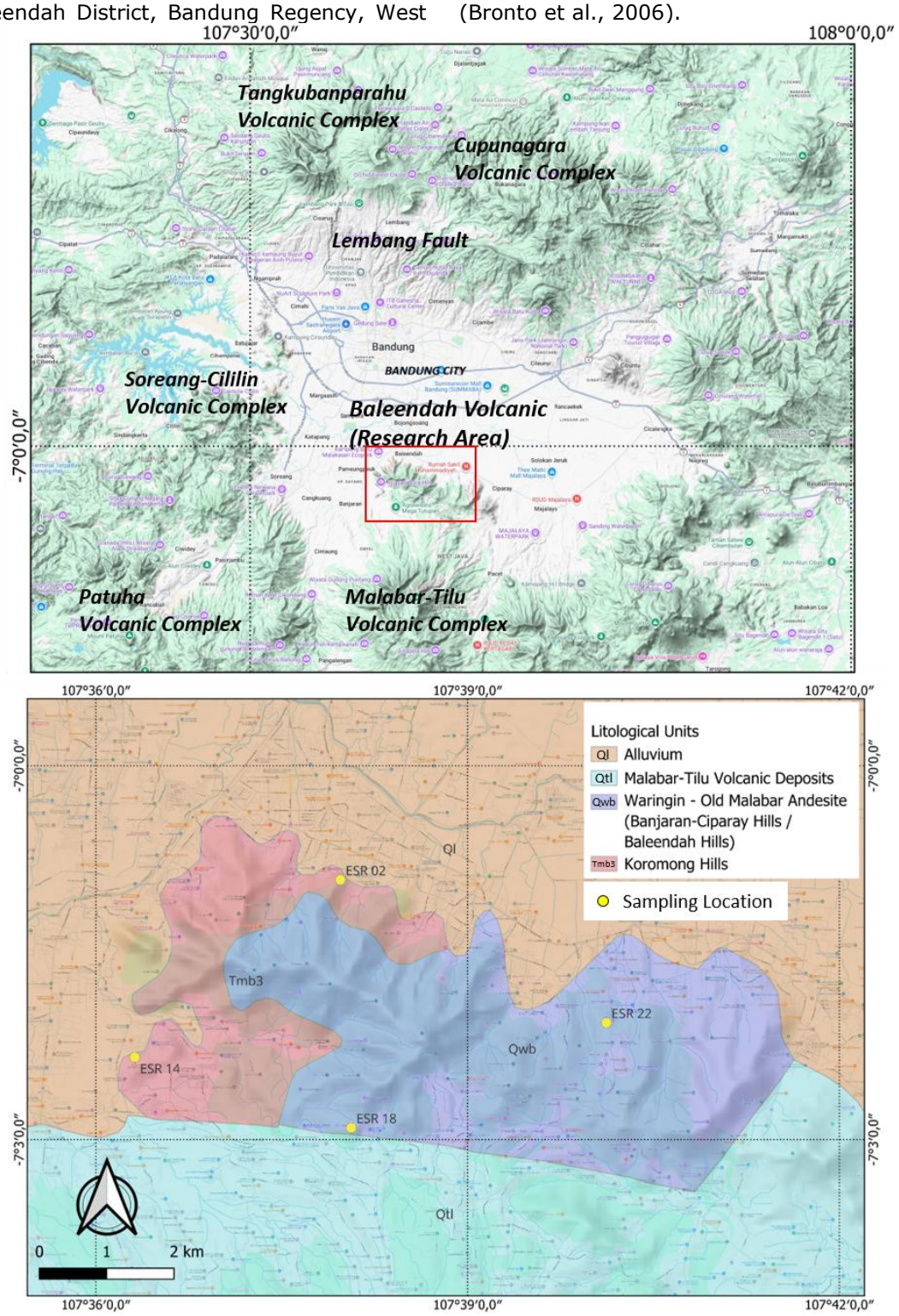

Figure 1. Map of Research Area. Yellow circle marks the location of the geochemistry samples.

Sunardi and Kimura (1998) published comprehensive geochemical data for late Cenozoic volcanic rocks around the Bandung Basin, including samples from the Pliocene of Kromong (KRM) and Cipicung (CPN), located in the southern mountain range approximately 10–15 km from the study area. Their work identified two co-existing magma series—tholeiitic and calc-alkaline—over the age range 4.1–0.05 Ma. Direct comparison between the ESR dataset and the Pliocene KRM and CPN suites of Sunardi and Kimura (1998) provides important temporal and petrogenetic context for understanding the evolution of Baleendah magmatism.

This study aims to characterise the geochemistry of volcanic rocks in the Baleendah area through XRF analysis of four representative samples, focusing on magma series identification, Harker variation diagrams, and petrogenetic implications within the broader context of West Java magmatism.

Regional Geology

The study area lies at coordinates 107°36′00"–107°40′40.8" E and 7°00′00"–7°03′36" S (Figure 1), within the volcanic hill zone of Southern Bandung (Bronto et al., 2006). Regional stratigraphy follows the Garut and Pameungpeuk Geological Map (Alzwar et al., 1992), comprising four units in ascending order: Beser Formation (Tmb, Late Miocene), Old Malabar Waringin-Bedil Andesite (Qwb, Pleistocene), Malabar Tilu Volcanic Rocks (Qmt, Pleistocene), and Lake Deposits (Qd, Holocene).

Within this regional framework, the Baleendah Volcanic Unit (BV), which is the primary subject of this study, corresponds to and is interpreted as part of the Malabar Tilu Volcanic Rocks (Qwb) unit. The BV records three eruptive phases: phase 1 (Gunung Bukitcula summit, 3.20 Ma), phase 2 (Gunung Geulis and Gunung Pipisan, 2.80 Ma), and phase 3 (Gunung Tikukur, 1,020 m a.s.l.). The unit is predominantly composed of interbedded andesitic lava flows with pyroclastic breccia intercalations (Bronto et al., 2006).

Tectonically, West Java is located at a convergent plate boundary where the Indo-Australian Plate subducts beneath the Eurasian Plate (Hamilton, 1979; Katili, 1973), generating the Sunda volcanic arc. The Wadati–Benioff zone beneath West Java lies at approximately 170 km depth (Sunardi and Kimura, 1998). The study area is dominated by the Java structural pattern, with east–west trending faults in the southern sector (Alzwar et al., 1992; Pulunggono and Martodjojo, 1994).

Petrological Characteristic

Consistent with previous petrographic descriptions of andesitic rocks from the Baleendah District (Soviati et al., 2017), the rocks are dark grey when fresh and brownish-grey when weathered, with a melanocratic–mesocratic colour index and porphyritic–aphanitic texture; columnar joint, sheeting joint, and autobreccia structures are present, with plagioclase, pyroxene, amphibole, and minor quartz visible in hand specimen. Thin section: hypocrystalline, inequigranular, ophitic, glomeroporphyritic, trachytic and vitrification textures; plagioclase (45–60%) as labradorite An50–60/andesine An45–50 with oscillatory/patchy zoning, sieve and resorption textures; pyroxene (5–15%) ophitic/subophitic; amphibole (3–10%) and biotite (1–3%) in distal samples; secondary quartz replacing groundmass, carbonate replacing plagioclase, secondary opaques, iron oxides.

METHODS

Field sampling was conducted at 16 observation stations across the Baleendah area. Four representative samples were selected based on their spatial position relative to the eruption source: ESR 18 (most proximal), ESR 22 and ESR 02 (intermediate), and ESR 14 (most distal). Sample selection prioritised fresh, unweathered material confirmed by hand specimen and thin section examination. Major-oxide and trace element concentrations were determined by X-Ray Fluorescence (XRF) spectrometry using fused glass beads for major oxides and pressed pellets for trace elements, following standard analytical procedures. Both major oxide and trace element data were therefore derived from the same XRF analytical session. Total iron was recalculated as FeOt using the conversion $FeOt = Fe_2O_3 \times 0.8998$. Rock classification was based on the Total Alkali–Silica (TAS) diagram of Middlemost (1994). Magma series affinity was assessed using three complementary approaches: (1) the SiO_2–K_2O diagram of Peccerillo and Taylor (1976); (2) the FeOt/MgO vs. SiO_2 diagram of Miyashiro (1974); and (3) the AFM triangular diagram of Irvine and Baragar (1971). Differentiation trends were assessed through Harker variation diagrams with SiO_2 as the differentiation index. Geochemical comparisons were made against Pliocene samples KRM and CPN from Sunardi and Kimura (1998).

RESULTS AND DISCUSSION

Major Oxide Composition

The complete XRF major oxide dataset is presented in Table 1. SiO_2 contents range from 57.60 to 63.27 wt.%, placing all samples in the intermediate compositional range. Al_2O_3 is notably high (15.78–19.48 wt.%), with the proximal sample ESR 18 recording the maximum value (19.48 wt.%), consistent with high-alumina andesite affinities typical of medium-K calc-alkaline arc magmas. MgO is uniformly low (0.62–1.36 wt.%), indicating that all samples represent evolved magmas that have undergone significant fractional crystallisation from a more mafic parental composition.

Total iron as FeOt ranges from 5.86 to 7.07 wt.%, with ESR 18 showing the highest value. CaO ranges from 5.03 to 6.80 wt.%, decreasing systematically from proximal to distal. Na_2O (3.37–3.84 wt.%) and K_2O (0.94–1.11 wt.%) are relatively stable, with K_2O slightly elevated in the most distal ESR 14 (1.11 wt.%). TiO_2 (0.52–0.63 wt.%) and P_2O_5 (0.16–0.21 wt.%) are uniformly low. LOI values (1.10–3.32 wt.%) are elevated in distal samples ESR 02 and ESR 14, indicating more pronounced post-magmatic alteration, which should be considered when interpreting mobile element trends.

Table 1. Major oxide composition of Baleendah volcanic rocks (wt.%) and comparison of ESR samples with the mean Pliocene KRM–CPN suite (Sunardi and Kimura, 1998).

Parameter	ESR 02	ESR 14	ESR 18	ESR 22	KRM–CPN[1]
SiO_2 (wt.%)	61.51	63.27	57.60	61.60	57.8–60.0
Al_2O_3 (wt.%)	16.50	15.78	19.48	17.52	17.5–18.2
MgO (wt.%)	1.32	0.62	1.36	1.10	2.8–3.4
CaO (wt.%)	5.33	5.03	6.80	5.73	6.9–7.8
FeOt (wt.%)	6.14	5.86	7.07	6.27	6.8–7.6
Na_2O (wt.%)	3.37	3.58	3.75	3.84	3.6-3.9
K_2O (wt.%)	0.95	1.11	0.96	0.94	1.0–1.4
TiO_2 (wt.%)	0.52	0.59	0.63	0.57	0.73–0.84
P_2O_5 (wt.%)	0.16	0.20	0.16	0.17	0.16-0.17
FeOt/MgO	4.65	9.45	5.20	5.70	2.1–2.9
Sr (ppm)	154	156	214	217	250–275
V (ppm)	100	76	110	108	140–155
Co (ppm)	23	18	26	21	24–26
Cr (ppm)	34	34	34	34	5–18
Rb (ppm)	25	~0	19	27	22–35
K_2O series	Calc-alk.	Calc-alk.	Calc-alk.	Calc-alk.	Calc-alk.
FeOt/MgO series	Tholeiitic	Tholeiitic	Tholeiitic	Trans.	Calc-alk.

$FeOt = Fe_2O_3 \times 0.8998$

Rock Classification

On the TAS diagram of Middlemost (1994) (Figure 2), the samples show a spread across the andesite–dacite boundary. The two proximal samples ESR 18 (SiO_2 = 57.60 wt.%) and ESR 22 (SiO_2 = 61.60 wt.%) plot within the andesite field, while ESR 02 (SiO_2 = 61.51 wt.%) and ESR 14 (SiO_2 = 63.27 wt.%) plot on or within the dacite field.

This geochemical classification, however, appears inconsistent with field and petrological observations, which indicate a uniform andesitic lithology across all four sample localities. The anomalously elevated SiO_2 in the distal samples ESR 02 and ESR 14 may be attributed to secondary silica enrichment associated with silicic glass in the groundmass, a phenomenon commonly observed in distal arc volcanic rocks that have undergone devitrification, hydrothermal alteration, or cryptic silicification.

The elevated LOI values in these same samples (3.06–3.32 wt.%) support the interpretation of post-magmatic alteration.

Accordingly, the rocks are interpreted as andesites on the basis of their petrographic characteristics and the composition of the less-altered proximal samples, with the TAS classification of the distal samples treated with caution.

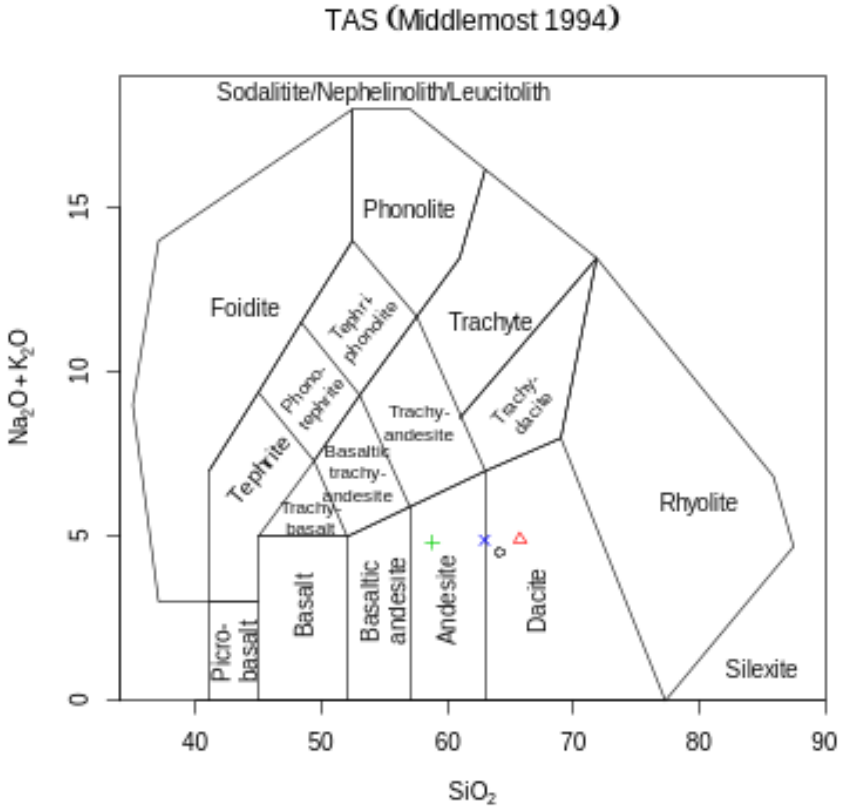

Figure 2. TAS diagram (Middlemost, 1994). ESR 18 and ESR 22 plot in the andesite field; ESR 02 and ESR 14 plot on or near the dacite boundary, likely reflecting secondary SiO_2 enrichment in distal samples.

Magma Series

Three discrimination diagrams are employed to assess magma series affinity. On the SiO_2–K_2O diagram of Peccerillo and Taylor (1976) (Figure 3), all four ESR samples plot within the medium-K calc-alkaline field (K_2O = 0.94–1.11 wt.%), consistent with subduction-related arc magmatism above the ~170 km Wadati–Benioff zone.

In contrast, the FeOt/MgO vs. SiO_2 diagram of Miyashiro (1974) (Figure 4) places three samples in the tholeiitic field, with ESR 14 transitional at the highest FeOt/MgO ratio (9.45). The AFM diagram (Figure 5) similarly shows iron-enrichment trending toward the F apex. FeOt/MgO ratios across the suite (4.65–9.45) substantially exceed the typical calc-alkaline range (<3.5).

This apparent duality of calc-alkaline on SiO_2–K_2O but tholeiitic-trending on FeOt/MgO and AFM is a recognised feature of evolved arc andesites. The K_2O classification reflects source mantle enrichment by slab fluids, while the elevated FeOt/MgO reflects iron accumulation during fractional crystallisation; the petrogenetic mechanism is discussed further in the Petrogenetic Implication section. The ESR suite is therefore best characterised as a medium-K calc-alkaline andesite with iron-enriched crystallisation trends.

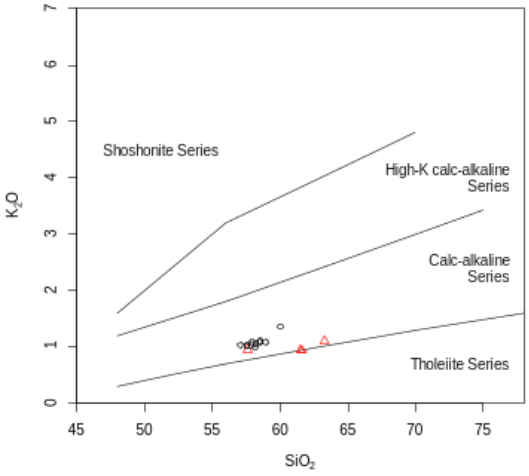

Figure 3. SiO_2–K_2O diagram (Peccerillo and Taylor, 1976). All ESR samples fall within the calc-alkaline series field, classifying them as medium-K calc-alkaline andesites.

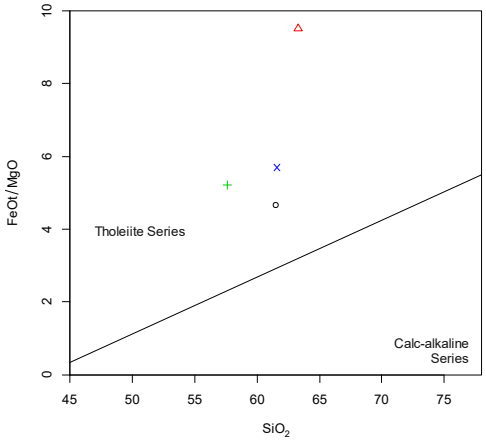

Figure 4. SiO_2 vs. FeOt/MgO diagram (Miyashiro, 1974). Dividing line between tholeiitic (TH) and calc-alkaline (CA) series after Miyashiro (1974). Most ESR samples plot in the tholeiitic field.

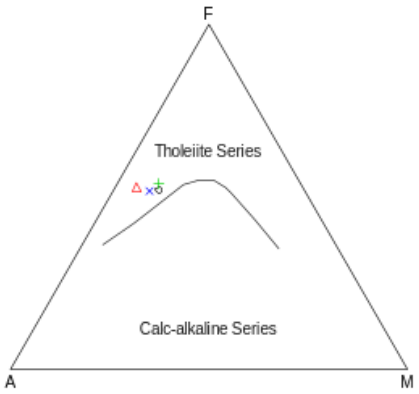

Figure 5. AFM diagram (Irvine and Baragar, 1971). ESR samples show enrichment of FeOt.

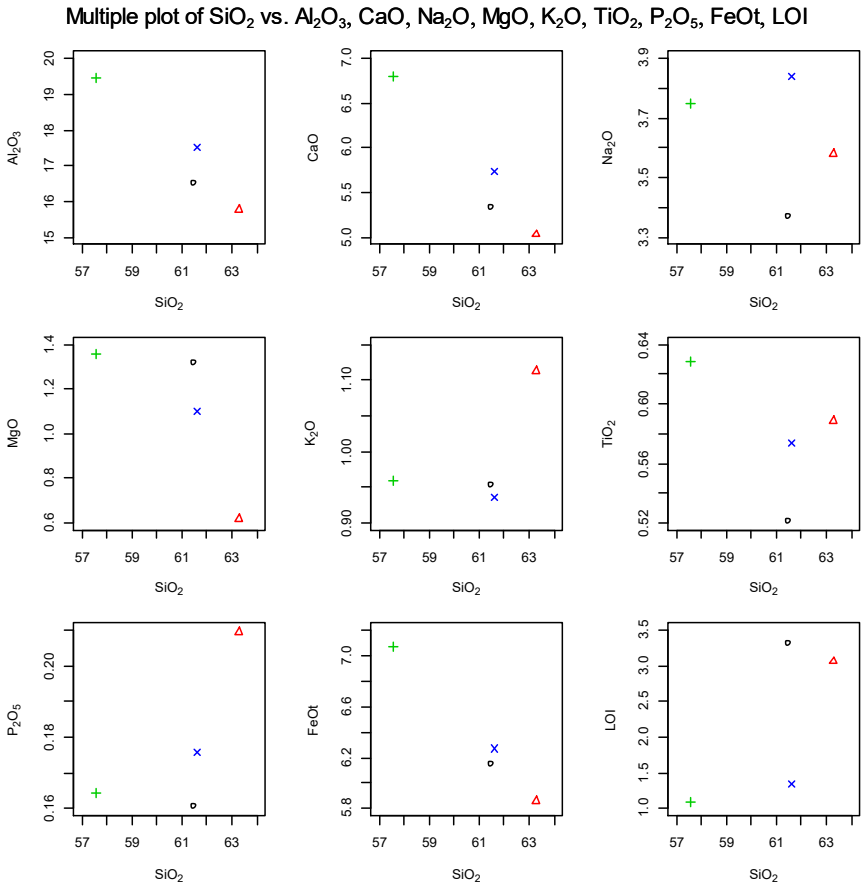

Figure 6. Harker variation diagrams including LOI and FeOt. Elevated LOI in ESR 02 and ESR 14 indicates post-magmatic hydrothermal alteration in distal samples.

Comparison with the Pliocene KRM–CPN Suite (Sunardi and Kimura, 1998)

Harker variation diagrams (Figure 6) show systematic decreases in Al_2O_3, CaO, MgO, and FeOt with increasing SiO_2, consistent with a coherent fractional crystallisation sequence. Elevated LOI in the distal samples ESR 02 and ESR 14 indicates post-magmatic hydrothermal alteration, which should be considered when interpreting mobile element trends.

The KRM (Kromong) and CPN (Cipicung) Pliocene samples of Sunardi and Kimura (1998) represent a well-documented calc-alkaline suite at 3.4–3.07 Ma from the southern mountain range of Bandung, approximately 10–15 km from the study area (Table 1). Sharing a similar arc-tectonic setting and broadly comparable age with the ESR phase 2 suite (~2.8–3.2 Ma), they provide an ideal reference for assessing geochemical evolution within the same volcanic system.

Both suites classify as calc-alkaline on the SiO_2–K_2O diagram, but diverge markedly in FeOt/MgO: the KRM–CPN suite yields values of 2.1–2.9, within the calc-alkaline range, whereas the ESR suite reaches 4.65–9.45, indicating more advanced iron enrichment. The ESR samples also show consistently lower MgO (0.62–1.36 vs. 2.8–3.4 wt.%), CaO (5.03–6.80 vs. 6.9–7.8 wt.%), Sr (154–217 vs. 250–275 ppm), V (76–110 vs. 140–155 ppm), Co (18–26 vs. 24–26 ppm), and TiO_2 (0.52–0.63 vs. 0.73–0.84 wt.%), reflecting more extensive fractionation of pyroxene, plagioclase, and Fe–Ti oxides. Notably, Cr in the ESR suite (~34 ppm) is higher than in KRM–CPN (5–18 ppm), possibly reflecting interaction with Cr-bearing lithospheric wall rocks during ascent or limited olivine fractionation.

Petrogenetic Implication

The combined geochemical evidence allows a coherent petrogenetic model to be constructed for the phase 2 Baleendah volcanic rocks. The calc-alkaline K_2O character, medium-K potassium contents, and tectonic position above the ~170 km deep Wadati–Benioff zone indicate that the parental magma originated by partial melting of a subduction-modified mantle wedge. Slab-derived aqueous fluids enriched in large-ion lithophile elements metasomatised the overlying mantle peridotite, lowering the solidus and triggering partial melting to generate a primary high-alumina basaltic andesite at depth, consistent with the model of Sunardi and Kimura (1998) for the broader Bandung Basin volcanic system.

Following segregation from the source, the primary melt ascended and underwent fractional crystallisation within a shallow crustal magma chamber. The proposed crystallisation sequence is: (1) early fractionation of calcic plagioclase and orthopyroxene, controlling the decreases in CaO, Al_2O_3, and MgO with increasing SiO_2; (2) fractionation of Fe–Ti oxide minerals (ilmenite, magnetite), which at low fO_2 is retarded relative to a high-fO_2 system, allowing FeOt to accumulate and producing the elevated FeOt/MgO ratios; and (3) late-stage sodic plagioclase fractionation, contributing to Sr depletion and Na_2O stabilisation. Petrographically observed sieve textures and resorption features in plagioclase phenocrysts indicate that the crystallisation history involved periodic episodes of magma recharge or decompression.

The critical difference between the ESR and KRM–CPN suites lies in the timing and extent of magnetite crystallisation. Sunardi and Kimura (1998) demonstrated that in the Bandung calc-alkaline suite, early magnetite crystallisation effectively buffers FeOt/MgO at low values (2.1–2.9). In the ESR suite, the higher FeOt/MgO and tholeiitic iron-enrichment trend indicate that magnetite crystallisation was delayed, possibly due to lower fO_2 or higher crystallisation temperature, allowing iron enrichment to proceed. This is consistent with a drier parental magma with lower dissolved water content; water content strongly controls both fO_2 and the stability of early magnetite in arc magmas (Gill, 1981). A lower degree of slab fluid flux into the mantle source for the ESR magma, perhaps reflecting waning fluid input between the Pliocene (KRM–CPN) and Late Pliocene (ESR) phases, could account for this difference.

Source depth estimates based on Hutchinson (1977) yield magma segregation depths of approximately 117–134 km, consistent with the ~170 km Benioff zone depth and a mantle wedge source. The comparable tectonic setting and SiO_2 range between ESR and KRM–CPN imply a broadly similar mantle source region, with the principal petrogenetic differences attributable to variations in magma water content and oxidation state during post-segregation crustal evolution.

CONCLUSION

Geochemical analysis of volcanic rocks from the Baleendah area yields the following conclusions:

1. All rocks are petrographically andesites; higher SiO_2 in distal samples on the TAS diagram reflects secondary silicification, not primary composition.
2. Medium-K calc-alkaline affinity on the SiO_2–K_2O diagram confirms a subduction-related origin, consistent with the Pliocene KRM–CPN suite.
3. Tholeiitic to transitional FeOt/MgO ratios (4.65–9.45) on the Miyashiro (1974) and AFM diagrams indicate iron enrichment under low oxygen fugacity.
4. Harker diagrams record coherent fractional crystallisation: decreasing Al_2O_3, CaO, MgO, and FeOt with increasing SiO_2.

5. Relative to KRM–CPN, the ESR suite shows lower compatible element concentrations and higher FeOt/MgO, reflecting a more evolved magma with de layed magnetite saturation.
6. The parental magma formed by partial melting of a metasomatised mantle wedge at ~117–134 km depth, differentiating in a shallow crustal chamber under lower fO_2.

ACKNOWLEDGEMENTS
The authors wish to thank the academic staff of the Faculty of Geological Engineering, Universitas Padjadjaran and the laboratory technicians who facilitated petrographic analyses.

REFERENSI

Alzwar, M., Akbar, N., Bachri, S., 1992. Geological Map of the Garut and Pameungpeuk Sheets, Java. Geological Research and Development Centre, Bandung.

Best, M.G., 2013. Igneous and Metamorphic Petrology. John Wiley and Sons, New York.

Bronto, S., Koswara, A., Lumbanbatu, K., 2006. Stratigrafi gunung api daerah Bandung Selatan, Jawa Barat. Indonesian Journal of Geology, 1(2), 89–101.

Gill, J.B., 1981. Orogenic Andesites and Plate Tectonics. Springer Verlag, Berlin–Heidelberg.

Hamilton, W., 1979. Tectonics of the Indonesian Region. USGS Professional Paper 1078.

Hutchinson, C.S., 1977. Granite emplacement and tectonic controls inferred from gravity data in Peninsular Malaysia. Tectonophysics, 42(2–4), T5–T16.

Irvine, T.N., Baragar, W.R.A., 1971. A guide to the chemical classification of the common volcanic rocks. Canadian Journal of Earth Sciences, 8(5), 523–548.

Katili, J.A., 1973. Geochronology of West Java and its implication on the theory of global tectonics. Tectonophysics, 19(3), 195–212.

Middlemost, E.A.K., 1994. Naming materials in the magma/igneous rock system. Earth-Science Reviews, 37(3–4), 215–224.

Miyashiro, A., 1974. Volcanic rock series in island arcs and active continental margins. American Journal of Science, 274(4), 321–355.

Peccerillo, A., Taylor, S.R., 1976. Geochemistry of eocene calc-alkaline volcanic rocks from the Kastamonu area, Northern Turkey. Contr. Mineral. and Petrol. 58, 63–81.

Pulunggono, A. and Martodjojo, S. 1994: Paleogene-Neogene tectonic changes are the most significant tectonic events in Java, Proceedings of Geology and Geotectonics of Java J s since the end of the Mesozoic to the Quaternary, Seminar of the 1st Department of Geology, Faculty of Engineering, UGM, 253-274.

Soviati, A.E., Syafri, I., Patonah, A., 2017. Petrogenesis of Andesite Bukit Cangkring, Jelekong Area, Baleendah District, Bandung Regency, West Java. Bulletin of Scientific Contribution: Geology, 1(2), 98–105.

Sunardi, E., Kimura, J., 1998. Temporal chemical variations in late Cenozoic volcanic rocks around The Bandung Basin, West Java, Indonesia. Journal of Mineralogy, Petrology and Economic Geology, 93, 103–128.

Wilson, M., 1989. Igneous Petrogenesis: A Global Tectonic Approach. Springer Netherlands, Dordrecht.